Chalcogenide Letters Vol. 18, No. 2, February 2021, p. 81 - 89

EFFECT OF ANNEALING ON THE STRUCTURE AND OPTICAL PROPERTIES OF LEAD SELENIDE AND CADMIUM SELENIDE THIN FILM PREPARED BY CHEMICAL BATH DEPOSITION

C. K. BANDOH, I. NKRUMAH*, F. K. AMPONG, R. K. NKUM, F. BOAKYE
Department of Physics, Kwame Nkrumah University of Science and Technology, Kumasi, Ghana

The effect of annealing on the structural and optical properties of lead selenide and cadmium selenide thin films prepared by chemical bath deposition has been studied. The films were annealed in air for a duration of 1 hour at temperatures of 673 K for CdSe and 573 K for PbSe. Both the as-deposited and annealed films were characterized by X-ray diffraction and optical absorption spectroscopy. The as–deposited CdSe films had the cubic structure with preferred orientation along (111) plane. However, after annealing there was a phase change from the cubic structure to the hexagonal structure with preferred orientation along the (002) plane. Both the as-deposited and annealed PbSe had the cubic structure with preferred orientation along the (200) plane. Other structural parameters such as the average crystallite size increased, whilst the dislocation density and strain decreased, suggesting a reduction in lattice imperfections after annealing. Optical absorbance of the films increased after annealing with a corresponding decrease in the direct band gap from 1.78 eV to 1.52 eV for CdSe, and 1.47 eV to 1.35 eV for PbSe. These results suggest an improvement in optical and structural properties after annealing.

(Received September 30, 2020; Accepted February 17, 2021)

Keywords: Chemical bath deposition, Cadmium Selenide, Lead Selenide, Annealing

1. Introduction

During the past few decades, there has been increasing interest in the deposition and characterization of group II–VI (ZnSe, CdS, CdTe, CdSe, etc.) and group IV – VI (PbS, PdSe, PbTe, etc.) binary semiconductor compounds, due to their wide application in various fields of science and technology. The exceptional optical, electrical and semiconducting properties of CdSe and PbSe thin films form the backbone of the electronic industry and the foundation of contemporary technology [1]. These exceptional semiconducting properties and their vast technological applications have been extensively reported in available literature.

An important technique in thin film fabrication, which can help enhance the properties of the thin film by changing the microstructure and phase, is post deposition annealing. Post deposition annealing of thin films can lead to significant changes in the structural, electrical, morphological and optical properties of semiconductor thin films [2]. The ability to tune the properties of a material by annealing may make it a better material with enhanced properties and performance.

Chemical Bath Deposition (CBD) offers a simple and inexpensive route to deposit binary and ternary semiconductor thin films, and is currently one of the fastest growing techniques of materials research. This deposition method is straightforward, inexpensive and yields high quality materials that are interesting for applications in various optical and electronic devices [3].

CBD is becoming an important deposition technique for thin films of compound materials like chalcogenides [4]. Another attractive feature of the CBD process is the ease with which alloys can be generated without the use of any sophisticated instrumentation and process control [5].

The effect of deposition time on the structural, morphological and optical band gap of lead selenide thin films synthesized by CBD, has been reported [6]. Effect of deposition temperature on the structural, morphological and optical band gap of lead selenide thin films synthesized by CBD,

* Corresponding author: inkrumah.sci@knust.edu.gh

https://doi.org/10.15251/CL.2021.182.81

has also been reported [7]. Hone et al. [8] reported the synthesis and characterization of CdSe nanocrystalline thin film deposited by the CBD technique and in another paper, reported the effect of annealing on the structural, morphological and optical band gap of nanocrystalline cadmium selenide thin films synthesized by CBD Technique [9].

This present study expounds how post-deposition annealing affects the various structural and optical properties of CdSe and PdSe thin films deposited by chemical bath deposition technique.

2. Experimental details

A simple chemical bath deposition method was employed to deposit CdSe and PbSe thin films onto glass substrates. Cadmium chloride, lead acetate and sodium selenosulphate (Na_2SeSO_3) were used as source of Cd^{2+}, Pb^{2+} and Se^{2-} respectively and ammonia as a complexing agent. Sodium selenosulphate was obtained by refluxing 19.5426 g of selenium powder with 30.2496 g of sodium sulphite (Na_2SO_3) in a refluxing equipment containing 500 ml distilled water and heated to 90° C for 6 hours.

2.1. Substrate preparation

The preparation of substrates is a crucial aspect that can contribute to film adherence [10]. It is therefore important that prior to the deposition of the semiconducting thin film the substrate, in this case microscope glass slide is cleaned completely to remove any undesirable substance from it. The microscope glass slides were left in nitric acid (HNO_3) for a few hours to remove any form of dirt, grease or other contaminants. They were then soaked in ethanol and later rinsed with de-ionized water before use.

2.2. Deposition of cadmium selenide (CdSe)

The chemical bath contained 5 ml of 0.5 M $CdCl_2$, 10 ml of 35 % NH_3, 45 ml of distilled water and 10 ml of 0.5 M Na_2SeSO_3. The pH of the resultant mixture was 11.61. The beaker containing the mixture was placed in a constant temperature bath kept at 80 ºC. The glass substrates were vertically immersed in the solution which was constantly stirred. The substrates were taken out after 60 minutes, washed with distilled water, and dried under ambient conditions before characterization.

2.3. Deposition of lead selenide (PbSe)

The deposition of PbSe started with 5 ml of 0.3 M $Pb(CH_3COO)_2.3H_2O$, 30 ml of 35 % NH_3, 30 ml distilled water and 5 ml of 0.3 M Na_2SeSO_3 in a 100 ml beaker. The pH of the mixture was 12.57. The temperature of the bath was also kept constant at 80 ºC. The glass substrates were vertically immersed in the solution which was constantly stirred. The deposition time for lead selenide was 15 minutes, after which the substrates were rinsed with distilled water and dried under ambient conditions.

It was observed that deposition occurred within the first 3 to 5 minutes and reached a limit of 15 minutes. Beyond this limit the films began to peel off from the substrate.

2.4. Post deposition annealing

The post deposition annealing processes were carried out in air at temperatures of 673 K for CdSe and 573 K for PbSe. The samples were introduced into the furnace, heated up to the set temperature and maintained for an hour after which the furnace was switched off and allowed to cool to room temperature. The samples were then taken out for further characterization.

The as-deposited CdSe thin films were red and well adhered to the substrates. The colour of the films changed from red to dark–brown after annealing.

The PbSe thin films obtained from the bath were uniform, mirror-like grey in colour and well adhered to the glass substrate before and after annealing. PbSe was annealed at 573 K because at 673 K, the films evaporated from the surface of the glass substrate.

2.5. Thin film characterization

The optical absorbance spectra of the films were measured at room temperature by a UV mini Schimadzu UV-VIS spectrophotometer (model: UV mini-1240) within a wavelength range of 300–1100 nm. During scanning, a blank glass slide was scanned first for base line correction. Subsequently, the coated microscope glass slides were scanned to obtain the absorbance spectra.

The crystal structure, orientation and chemical composition of the thin films were determined with an Empyrean Series 2 PANalytical X–ray diffractometer with monochromatic CuKα source radiation (1.54060 Å). The diffractometer was operated in the step scan mode with a step size of 0.08 in the 2θ range of 20–70 ^{o}. The accelerating voltage and current were 45 kV and 40 mA respectively.

3. Results and discussion

3.1. Cadmium selenide, CdSe

3.1.1. X-ray diffraction analysis

X–ray diffractograms of CdSe thin films for as–deposited and annealed films are shown in Fig. 1. The presence of several peaks in the diffractogram confirm the polycrystalline nature of the films [11]. In Fig. 1, the peaks at 2θ positions 25.56 ^{o}, 42.35 ^{o} and 50.01 ^{o} are indexed to reflections from the (111), (220) and (311) planes of the cubic CdSe phase [ICDD, 98–062–0416] respectfully. However, after annealing, there was a change from the cubic phase of CdSe with preferred orientation along the (111) plane to the hexagonal phase of CdSe with preferred orientation along the (002) plane. The peaks observed at 2θ positions 23.78 ^{o}, 25.27 ^{o}, 26.98 ^{o}, 34.97 ^{o}, 41.88 ^{o}, 45.74 ^{o} and 49.60 ^{o} were indexed to reflections from the (100), (002), (101), (102), (110), (103) and (112) planes of the hexagonal CdSe [ICDD, 98–062–0423]. The annealed sample also showed the presence of a single low intensity peak at 2θ position 30.25 ^{o} which corresponds to the (021) plane of the cubic $CdSe_2$ (cadmium perselenide) phase [ICDD, 98-062-0416].

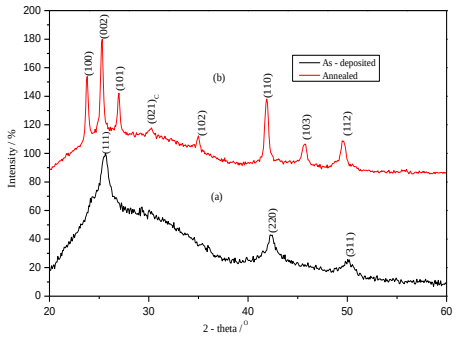

Fig. 1. X - ray diffraction data for CdSe (a) as-deposited and (b) annealed at 673 K.

According to Hodes [4], the energy difference between the hexagonal (wurtzite) and cubic (zincblende) phases is very small (the former is slightly more stable). The relative intensity of the (002) reflection is high, indicating the deposits are oriented with the c-axis perpendicular to the substrate [12]. The results of annealing significantly depend on its kinetics: the rate of heating and cooling and time of exposure at a given temperature. It is worth noting that in our previous report by Hone et al. [9]. X-ray diffraction analysis revealed that after annealing in air at a temperature of 350 ^{0}C for one hour, CdSe thin films had three major peaks corresponding to the cubic structure with preferred orientation along the (111) plane. There was no evidence of the presence of the hexagonal phase.

3.1.2. Determination of the average grain size

The average grain sizes of both the as–deposited and annealed CdSe samples were determined from the X – ray diffraction data using the Scherrer's formula which is given as;

$$D = \frac{0.9\lambda}{\beta cos\theta} \quad (1)$$

where D is crystallite size, λ is wavelength of the X–ray used, β is the full width at half maxima (FWHM) in radian and θ is the Bragg's angle.

The average grain sizes were found to be 6.3 nm and 33.6 nm for as–deposited and annealed at 673 K respectively. According to Hodes [4], thin films annealed at temperatures above 573 K usually exhibited a large degree of crystal growth and this might explain the increase in the observed grain size.

3.1.3. Strain and dislocation density

The dislocation density which is a measure of defects in the crystallite [13], was determined using the Williamson and Smallman's formula [14]:

$$\delta = \frac{n}{D^2} \quad (2)$$

where *n* is a factor, when equal to unity gives a maximum dislocation density and *D* is the average crystallite size.

The microstrain developed in the films was also calculated using the relation [15]:

$$\varepsilon = \frac{\beta cos\theta}{4} \quad (3)$$

Dislocation density and strain of both the as-deposited and the annealed samples were determined using the most intense peak of the X-ray diffraction pattern.

The structural parameters obtained for CdSe have been summarized in Table 1.

From Table 1, it can be observed that strain and dislocation density decreased with annealing. This may be as a result of the increase in average crystallite size which indicates a lower number of lattice imperfections [16].

Table 1. Structural parameters of CdSe thin films.

CdSe Samples	**2θ in degree**	**hkl**	**d-spacing**	**Average Crystallite size(nm)**	**Strain(ε) lines^{-2}m^{-4}**	**Dislocation density (δ) lines/m^2**
As-deposited	25.56	111	3.484	6.3	5.50×10^{-3}	2.52×10^{16}
	42.53	220	2.134			
	50.01	311	1.824			
Annealed	23.78	100	3.742	33.6	1.03×10^{-3}	8.86×10^{14}
	25.27	002	3.524			
	26.98	101	3.303			
	34.97	102	2.564			
	41.88	110	2.155			
	45.74	103	1.952			
	49.60	112	1.836			

3.2. Optical absorption

Fig. 2 shows the absorption spectra of the CdSe thin films before and after annealing at a temperature of 673 K in air for 1 hour

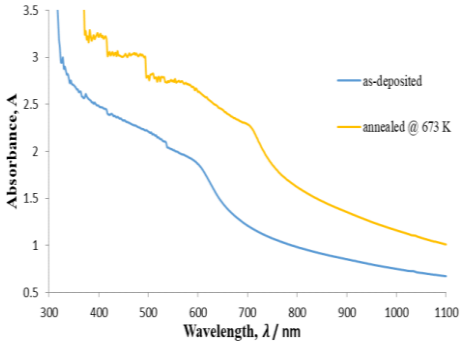

Fig. 2. A plot of Absorbance against Wavelength for the as-deposited and annealed CdSe films.

The films show a marginal increase in absorbance after annealing. Similar behaviour was observed by Nawfal et al. [17] and Moradian et al. [18] who attributed it to an increase in grain size. Generally, the optical properties of semiconductors, especially the absorption spectra and optical band gaps, are intensively affected by their band structure, which is basically dominated by the microstructure [19].

It can be observed from the optical spectra that the fundamental absorption edge shifts towards longer wavelengths (red shift) after annealing. This red shift together with an increase in absorbance after annealing may be attributed to an increase in grain size which was confirmed by the XRD analysis. Red shift has also been attributed to photoelectrochemical reactions that occur at the surface of the crystal [4].

3.2.1. Determination of optical band gap

From the absorption spectra, the optical band gaps of the films were determined using the Stern [20] relation given as:

$$A = \frac{[K(h\upsilon - E_g]^{n/2}}{h\upsilon} \tag{4}$$

where A is the absorbance, υ is the frequency, h is the Planck's constant, *K* is a constant whiles *n* carries the value of either 1 or 4, for direct and indirect transitions respectively. Almost all the II–VI compounds are direct band gap semiconductors [21], thus n is taken as 1. By plotting $(Ah\upsilon)^{2/n}$ versus *hν*, the energy band gap is obtained by fitting a line to the linear portion of the graph and extrapolating the fitted line to the point where it intersects the *hν* axis [3] as shown in Fig. 3.

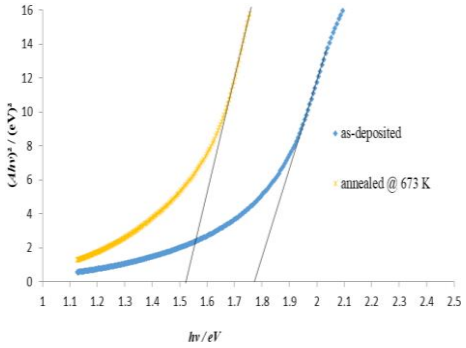

Fig. 3. Plot of $(Ah\upsilon)^2$ versus hυ for CdSe thin film as- deposited and annealed.

The linear nature of the plots for n = 1 indicates the existence of direct transitions. The band gap of the films was determined to be 1.78 and 1.52 eV respectively for the as–deposited and

annealed film. The decrease in band gap from 1.78 eV to 1.52 eV after annealing could be attributed to variations in the microstructure as evidenced from Table 1. Nawfal et al. [17] reported a decrease in band gap from 2.0 eV to 1.7 eV with increasing annealing temperatures and attributed it to an increase in grain size which results in a decrease in grain boundaries. They also observed a colour change from red–orange (for as–deposited) to dark–brown after annealing at 673 K. A similar colour change was observed in this work.

3.3. Results for lead selenide

3.3.1. X-Ray Diffraction Patterns of the PbSe

The diffraction pattern of as–deposited and annealed PbSe thin films are shown in Fig. 4. The appearance of several peaks in the diffractogram suggests that the PbSe thin films are polycrystalline in nature. The as–deposited films showed seven peaks at 2θ positions 25.11 °, 28.50 °, 41.59 °, 49.20 °, 51.55 °, 60.22 ° and 68.23 ° which correspond to reflections from the (111), (200), (220), (311), (222), (400) and (420) planes of the cubic PbSe phase [ICDD, 01–078–1903]. Unlike CdSe, PbSe showed no phase change after annealing. The XRD pattern of the annealed film also showed seven peaks at 2θ positions 25.15 °, 29.07 °, 41.64 °, 49.29 °, 51.65 °, 60.44 ° and 68.58 ° which correspond to the (111), (200), (220), (311), (222), (400) and (420) planes of the cubic PbSe [ICDD, 01–078–1903]. From the X–ray diffractograms, the preferred orientation of PbSe thin films is along the (200) plane. The intensity and number of diffraction peaks increased after annealing, indicating a considerable improvement in the crystalline nature of the PbSe thin film [7]. The diffraction patterns also show a shift in peak positions of the annealed samples towards higher angles indicating a contraction of the lattice [12].

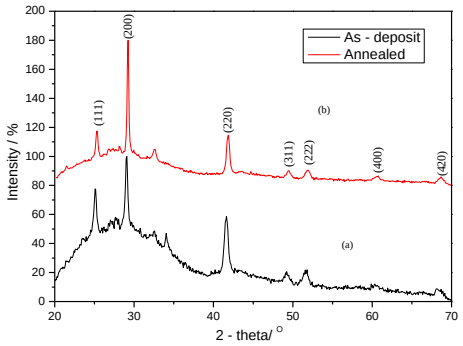

Fig. 4. X - ray diffraction data for PbSe as-deposited and annealed at 573 K.

It can be observed from the XRD spectra that the intensity of the peak indexed to (200) plane for the annealed sample is relatively higher than that of the as–deposited sample. This increase in peak intensity is an indicative of temperature induced grain growth along the (200) plane [22]. The average crystallite size was calculated from a full width at half maximum of the most intense diffraction peak using the Debye–Scherrer's formula [23]. The average crystallites size of the as–deposited and the annealed samples were found to be 10.3 nm and 21.4 nm respectively.

The lattice constant "*a*" (for cubic structure) was calculated using the relation:

$$a = d\sqrt{h^2 + k^2 + l^2} \tag{5}$$

The lattice constant was found to decrease slightly from 6.259 Å to 6.139 Å for as–deposited and annealed at 573 K respectively. Dislocation density (δ) and microstrain (ε) for both the as-deposited and the annealed PbSe were calculated using equations 2 and 3 respectively. Dislocation density and microstrain were determined from the (200) plane. The results obtained are summarized in Table 2.

From Table 2, it can be observed that dislocation density and strain decreased with annealing. This may be as a result of the increase in average crystallite size after annealing, which

indicates a lower number of lattice imperfections [16] and formation of high quality thin films [15].

Table 2. Structural parameters of PbSe thin films.

PbSe Samples	2θ in degree	hkl	d-spacing	Average Crystallite size(nm)	Strain(ε) lines^{-2}m^{-4}	Dislocation density (δ) lines/m^2
As-deposited	25.11	111	3.54	10.3	3.46×10^{-3}	9.43×10^{15}
	28.50	200	3.13			
	41.59	220	2.17			
	49.20	311	1.85			
	51.55	222	1.77			
	60.22	400	1.54			
	68.23	420	1.37			
Annealed	25.15	111	3.54	21.4	1.68×10^{-3}	2.18×10^{15}
	29.07	200	3.07			
	41.64	220	2.17			
	49.29	311	1.85			
	51.65	222	1.77			
	60.44	400	1.53			
	68.58	420	1.37			

3.3.2. Optical absorption

Spectral dependence of absorbance as a function of wavelength for as–deposited and annealed PbSe thin films are shown in Fig. 5.

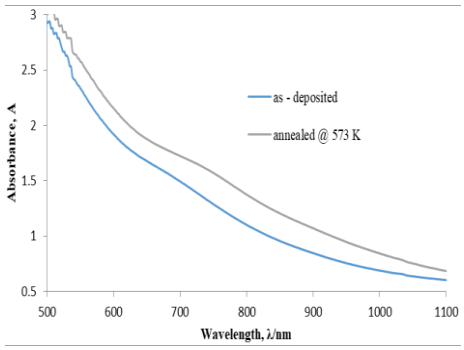

Fig. 5. A plot of Absorbance against Wavelength for PbSe as-deposited and annealed.

The films showed an increase in absorbance after annealing. It can be observed that the fundamental absorption edge shifts towards longer wavelength after annealing temperatures (red shift), indicating a reduction in band gap. Increase in absorbance with annealing may be due to an increase in grain size and a decrease in density of defect states [16], as evidenced from Table 2

3.4.3. Determination of optical band gap

From the absorption spectra, the optical band gaps of the films were determined using the Stern (1963) relation for near absorption edge.

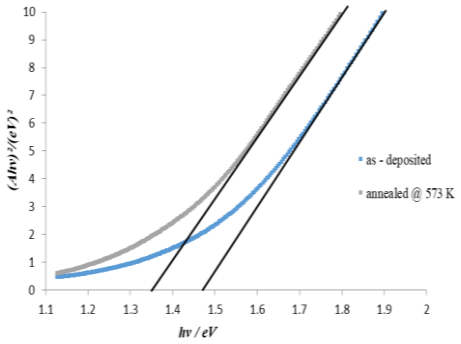

Fig. 6. Plot of $(Ahυ)^2$ against hυ for PbSe thin film as- deposited and annealed at 573 K.

The linear nature of the plots in Fig. 6, for n = 1 indicate the existence of direct transitions. The band gap of the films was found to be 1.47 eV and 1.35 eV for as–deposited and annealed respectively. Similar band gaps have been reported by Kassim et al. [24], Jadhav and Khairnar [25] and Ghobadi et al [26]. The observed decrease in band gap after annealing, may be attributed to the variation of the lattice constant, average crystallite size, strain and dislocation density [7], as evidenced from Table 2.

4. Conclusion

A study has been carried out to determine the effect of annealing on the crystal structure and optical properties of chemical bath deposited, lead selenide and cadmium selenide thin films. The duration for annealing was 1 hour at temperatures of 673 K for CdSe and 573 K for PbSe. Both the as-deposited and annealed films were characterized by X-ray diffraction and optical absorption spectroscopy. The as–deposited CdSe films had the cubic structure with preferred orientation along (111) plane. However, after annealing there was a phase change from the cubic structure to the hexagonal structure with preferred orientation along the (002) plane. The XRD results revealed a polycrystalline cubic structure of PbSe with preferred orientation along the (200) plane. There was no phase change in PbSe after annealing. The pattern of prominent peaks in both samples showed an increase in intensity after annealing indicating an improvement in crystallinity.

The average crystallites size of CdSe increased from 6.3 nm to 33.6 nm after annealing whilst PbSe also showed an increase in average crystallite size from 10.3 nm to 21.4 nm after annealing. Other structural parameters such as strain and dislocation density, in both films, decreased after annealing. These together with the increase in crystallite size is an indication of better crystallinity in the annealed samples. Optical analysis showed a decrease in the direct band gap of CdSe, from 1.78 eV for as–deposited to 1.52 eV after annealing, whiles that of PbSe decreased from 1.47 eV to 1.35 eV after annealing which also suggests better crystallinity. The results from all the characterization techniques used, suggest an improvement in the crystal structure and optical properties of the thin films after annealing.

References

[1] H. M. Ali, S.A Saleh, Thin Solid Films **556**, 552 (2014).
[2] M. H. Kabir, M. M. Ali, M. A. Kaiyum, M. S. Rahman, Journal of Physics Communications **3** (105007), 1 (2019).
[3] I. Nkrumah, F. K. Ampong, B. Kwakye-Awauh, T. Ive, Journal of Advances in Physics **11**(1), 2954 (2015).
[4] G. Hodes, Chemical Solution Deposition of Semiconductor Films, Marcel Dekker Inc, New York, **4** (2002).
[5] M. A. Barote, A. A. Yadav, E. U. Masumdar, Chalcogenide Letters **8**(2), 129 (2011).

[6] F. G. Hone, F. K. Ampong, T. Abza, I. Nkrumah, M. Paal, R. K. Nkum, F. Boakye, Materials Letters **155**, 58 (2015).
[7] F. G. Hone, F. K. Ampong, Materials Chemistry and Physics **183**, 320 (2016).
[8] F. G. Hone, F. K. Ampong, T. Abza, I. Nkrumah, R.K. Nkum, F. Boakye, International Journal of Thin Film Science and Technology **4**(2), 69 (2015).
[9] F. G. Hone, F. K. Ampong, I. Nkrumah, R. K. Nkum, F. Boakye, Elixir Thin Film Technology **84**, 33486 (2015).
[10] V. Edelson, Brown Alumni Magazine, 1 (2007).
[11] S. R. Vishwakarma, A. Kumar, S. Prasad, R. S. Tripathi, Chalcogenide Letters 1**0**(10), 393 (2013).
[12] F. K. Ampong, J. A. Awudza, R. K. Nkum, F. Boakye, P. J. Thomas, P. O'Brien, Solid State Sciences **40**, 50 (2015).
[13] C. Rajashree, A. R. Balu, V.S. Nagarethinam, International Journal of ChemTech Research **6**(1), 347 (2014).
[14] G. K. Williamson, R. E. Smallman, Philosophical Magazine **1**(1), 34 (1956).
[15] M. R. Bhuiyan, M. Azad, S. M. Hasan, Indian Journal of Pure & Applied Physics **49**, 180 (2011).
[16] A. Begum, A. Hussain, A. Rahman, Beilstein Journal of Nanotechnology **3**(1), 438 (2012).
[17] Y. J. Nawfal, T. M. Marwa, A. M. Noor, Rafidain Journal of Science **23**(1), 116 (2012).
[18] R. Moradian, N. Ghobadi, M. Roushani, M. Shamsipur, Journal of Iranian Chemical Society **8**, S104 (2011).
[19] Z. Feng-Ling, L. Xiao-Min, G. Xiang-Dong, Q. Ji-Jun,. Journal of Inorganic Materials **24**(4), 778 (2009).
[20] K. Anuar, W. T. Tan, M. Jelas, S. M. Ho, S.Y. Gwee, Thammasat International Journal of Science & Technology **15**(2), 64 (2010).
[21] V. Kumar, M. K. Sharmam, J. Gaur, T. P. Sharmam, Chalcogenide Letters **5**(11), 289 (2008).
[22] T. S. Shyju, S. Anandhi, R. Sivakumar, S. K. Garg, R. Gopalakrishnan, Journal of Crystal Growth **353**(1), 47 (2012).
[23] F. G. Hone, F. K. Ampong, T. Abza, I. Nkrumah, R.K. Nkum, F. Boakye, Elixir Thin Film Technology **76**, 28432 (2014).
[24] A. Kassim, T. W. Tee, H. S. Min, S. Monohorn, S. Nagalingam, Kathmandu University Journal of Science, Engineering and Technology **6**(2), 126 (2010).
[25] S. R. Jadhav, U. P. Khairnar, Archives of Applied Science Research **4**(1), 169 (2012).
[26] N. Ghobadi, P. Sohrabi, G. Haidari, S. S. Haeri, Journal of Interfaces, Thin Films and Low Dimension Systems **2**(1), 139 (2019)